THE JOURNAL OF PHYSICAL CHEMISTRY Letters

Letter

pubs.acs.org/JPCL

Role of Small Pd Ensembles in Boosting CO Oxidation in AuPd Alloys

Hyung Chul Ham,[†] J. Adam Stephens,[†] Gyeong S. Hwang,*[,†] Jonghee Han,[‡] Suk Woo Nam,[‡] and Tae Hoon Lim[‡]

[†]Department of Chemical Engineering, The University of Texas at Austin, Texas 78712, United States

[‡]Fuel Cell Research Center, Korea Institute of Science and Technology (KIST), Seoul, Korea

Supporting Information

ABSTRACT: We present a theoretical explanation on how PdAu alloy catalysts can enhance the oxidation of CO molecules based on density functional theory calculations of CO adsorption and oxidation on AuPd/Pd(111) surfaces. Our study suggests that the enhanced activity is largely attributed to the possible existence of "partially-poisoned" Pd ensembles that accommodate fewer CO molecules than Pd atoms. Whereas the oxidation of preadsorbed CO is likely governed by O_2 trapping, our study shows that small Pd ensembles such as dimers and compact trimers tend to provide more active sites than larger ensembles; CO adsorbed on a Pd monomer is found to react hardly with O_2 to form CO_2. In addition, we find the tendency of CO-induced Pd agglomeration, which may in turn facilitate CO oxidation by creating more dimers and compact trimers as compared with the adsorbate-free surface where monomers are likely prevailing.

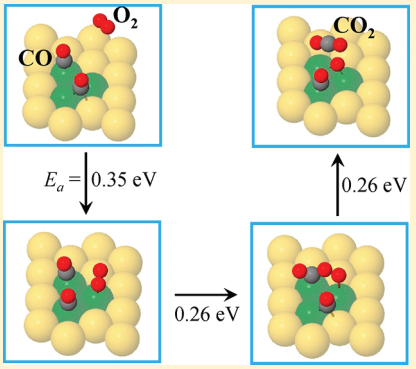

SECTION: Surfaces, Interfaces, Catalysis

Many noble metal-based catalysts are susceptible to activity loss due to carbon monoxide (CO) poisoning, in which CO molecules tightly bind to active sites.[1−5] In particular, CO poisoning of platinum (Pt)-based electrocatalysts in proton exchange membrane fuel cells is a serious problem, which has drawn much interest in developing CO-tolerant non-Pt catalysts. Palladium (Pd) is considered to be a viable alternative to Pt because it is more abundant and less expensive and also has a higher CO tolerance, in addition to showing similar catalytic behavior and long-term durability in acidic media. Furthermore, a series of recent studies[1,2,6,7] has provided evidence that alloying Pd with other metals can lead to considerable enhancements in catalytic activity and CO tolerance.

For instance, alloys of Pd with gold (Pd−Au) have been found to exhibit a greater resistance to CO poisoning than pure Pd. Whereas the CO-tolerance mechanism is still unclear, in oxidation catalysis we think it is possible that CO poisoning can be mitigated through the catalytic oxidation of CO to CO_2. Pd−Au alloy catalysts have been recently demonstrated to boost CO oxidation even at low temperatures.[2] For Pd−Au catalysts, the surface distribution of Pd and Au atoms likely plays a critical role in determining their catalytic properties. Recent studies have suggested that contiguous Pd atoms are necessary for CO oxidation,[8] whereas isolated Pd atoms are mainly responsible for the observed high selectivity in the direct H_2O_2 synthesis.[9]

In this Letter, we present a first-principles study of Pd ensemble size and shape on the surface activity of AuPd/Pd(111) toward the oxidation of preadsorbed CO with O_2. We first examine the adsorption structure and energetics of CO on various Pd ensembles and then the trapping and activation of O_2 in the vicinity of preadsorbed CO, followed by calculations of the pathways and barriers for the reaction between coadsorbed CO and O_2. Our study unequivocally demonstrates that the CO + O_2 reaction is very sensitive to the arrangement of Pd surface atoms; small Pd ensembles such as dimers and compact trimers are expected to provide more active sites than larger ensembles, whereas Pd monomers are highly unlikely to catalyze the CO oxidation reaction. We also discuss how CO adsorption may affect the distribution of Pd ensembles and consequently the catalytic oxidation of CO with O_2.

The calculations reported herein were performed on the basis of spin polarized density functional theory (DFT) within the generalized gradient approximation (GGA-PW91),[10] as implemented in the Vienna ab-initio simulation package (VASP).[11] The projector-augmented wave (PAW) method[12] with a planewave basis set was employed to describe the interaction between core and valence electrons. The valence configurations employed to construct the ionic pseudopotentials are: $5d^{10}$ $6s^1$ for Au, $4d^9$ $5s^1$ for Pd, $2s^2$ $2p^2$ for C, and $2s^2$ $2p^4$ for O. An energy cutoff of 350 eV was applied for the planewave expansion of the electronic eigenfunctions.

For a model surface, we used a supercell slab that consists of a rectangular $2\sqrt{3} \times 4$ surface unit cell with four atomic layers, each of which contains 16 atoms. As illustrated in Figure 1, the bottom three layers are pure Pd, and the topmost layer is a

Received: December 1, 2011
Accepted: February 6, 2012

   dx.doi.org/10.1021/jz201585q | J. Phys. Chem. Lett. 2012, 3, 566−570

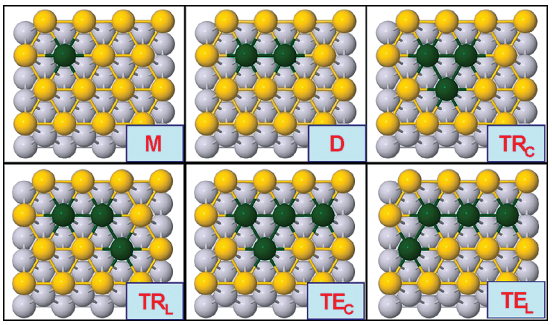

Figure 1. Model PdAu surfaces considered in this work, Pd monomer (indicated as M), dimer (D), compact trimer (TR_C), linear trimer (TR_L), compact tetramer (TE_C), and linear tetramer (TE_L). The green, gray, and gold balls represent surface Pd, subsurface Pd, and Au atoms, respectively.

PdAu alloy that contains one of the small Pd ensembles examined: monomer (indicated by M throughout the paper), dimer (D), linear trimer (TR_L), compact trimer (TR_C), linear tetramer (TE_L), and compact tetramer (TE_C). The slab is separated from its periodic images in the vertical direction by a vacuum space corresponding to seven atomic layers. Whereas the bottom two layers of the four-layer slab were fixed at Pd bulk positions, the upper two layers were fully relaxed until residual forces on all constituent atoms became smaller than 5×10^{-2} eV/Å. For the Brillouin zone integration, we used a $(2 \times 2 \times 1)$ Monkhorst-Pack mesh of k points to determine the optimal geometries and total energies of the systems examined, and increased the k-point mesh size up to $(7 \times 7 \times 1)$ to refine their electronic structures. Reaction pathways and barriers were determined using the climbing-image nudged elastic band method (CI-NEB)[13] with eight intermediate images for each elementary step. Previous studies[9,14] demonstrated the calculation conditions chosen to be sufficient for describing the Pd ensemble effect on the surface reactivity of the AuPd alloy considered.

In this work, we assume that CO oxidation occurs via a Langmuir–Hinshelwood (LH) type reaction; that is, coadsorption of CO and O_2 precedes CO oxidation. Note that CO oxidation on typical transition-metal surfaces including Pd and AuPd has been shown to follow the LH mechanism.[2,15,16] To study CO oxidation on AuPd in detail, it is necessary to determine likely adsorption configurations of the reactants. For CO, we considered three types of adsorption sites: on-top (T), bridge (B), and hollow (H). On-top sites are located directly above surface atoms, and bridge sites are situated midway between nearest-neighbor pairs of surface atoms. Hollow sites lie on the three-fold axes at the centers of groups of three surface atoms. At T, B, and H sites on pure Pd(111), CO adsorption energies are predicted to be 1.42, 1.87, and 2.05 eV, respectively; for comparison, CO adsorption energies were also calculated on Au/Pd(111) and turn out be much smaller (<0.25 eV) at all three types of site. This clearly demonstrates that CO binds strongly to the Pd surface and also that the adsorption energy greatly depends on adsorption site type, which is consistent with previous studies, although the predicted adsorption energies are rather sensitive to the choice of the exchange-correlation functional.[17]

On the AuPd/Pd(111) surface alloy, our calculations suggest that adsorption of CO to mixed Au–Pd bridge and hollow sites is unstable. For example, a CO molecule initially placed at a B site between a Pd monomer and a neighboring Au atom will spontaneously "stand up" to assume an on-top orientation on the Pd atom. For these reasons, we considered only T, B, and H sites in the AuPd surface alloy, which are fully coordinated by Pd. Owing to differences in their sizes and shapes, every Pd ensemble in the AuPd(111) surface hosts a different assortment of T, B, and H sites that meet this criterion. The monomer, which is completely surrounded by its six Au neighbors, provides only an on-top site. The dimer (D), linear trimer (TR_L), and linear tetramer (TE_L) contain not only on-top sites but also bridge sites between their adjacent Pd atoms. The compact trimer (TR_C) and compact tetramer (TE_C) host sites of all three types.

Figure 2 shows the minimum-energy CO adsorption configurations with increasing degrees of coverage up to one

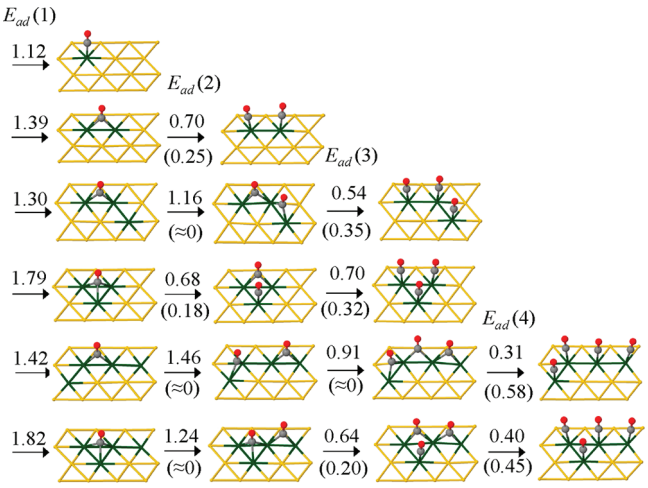

Figure 2. Calculated energy gains and activation barriers (in parentheses) for each configuration during the CO adsorption process on different Pd ensembles. All energy values are given in electronvolts. Note that at each configuration the barrier for CO desorption can be approximated by the sum of corresponding energy gain upon adsorption and adsorption activation barrier. Yellow and green wireframes represent surface Au and Pd atoms, respectively, and red and gray balls indicate respective O and C atoms in CO molecules.

CO per Pd atom for different Pd ensembles. Here the adsorption energy of the nth molecule to adsorb on a Pd ensemble $[E_{ad}(n)]$ is given by: $E_{ad}(n) = -[E_{ad}(n\text{CO}) - E_{ad}((n-1)\text{CO}) - E(\text{CO})]$, where $E_{ad}(n\text{CO})$ and $E(\text{CO})$ are the total energies of the most stable n absorbed Pd ensemble and the gas-phase CO, respectively. The adsorption energies [site-type] of a single CO molecule are predicted to be 1.12 eV [M(T)], 1.39 eV [D(B)], 1.42 eV [TR_L(B)], 1.79 eV [TR_C(H)], 1.42 eV [TE_L(B)], and 1.82 eV [TE_C(H)]. Note that the adsorption energies follow the same trend in site-dependence exhibited by the pure Pd(111) surface, T < B < H; the H sites (on TR_C and TE_C) are on average about 0.44 and 0.69 eV more favorable than the B sites (on D, TR_L, and TE_L) and the T site (M), respectively. Furthermore, the two H-site adsorption energies are almost identical, whereas the three B-site energies fall within a range of only ~0.1 eV. The results clearly indicate that the CO adsorption strength is mainly determined by whether the Pd ensembles, by virtue of their size and shape, host H, B, or only T sites.

As the CO coverage increases, the adsorption energies are seen to decline. This is partially because of the gradual lack of favorable adsorption sites; that is, an energy penalty must be

dx.doi.org/10.1021/jz201585q | J. Phys. Chem. Lett. 2012, 3, 566–570

paid to rearrange already-absorbed CO to less favorable absorption sites to accommodate the addition of more CO. For example, CO absorbed to the H site on TR_C must shift to a less favorable B site to permit a second adsorption. CO−CO and CO−surface−CO interactions also affect the CO adsorption strength but turn out to be less important than the adsorption site dependence. On the basis of the configurations, we also calculated activation barriers for adsorption and desorption at each level of CO coverage. As shown in Figure 2, in all cases, desorption is a thermally activated process with large enthothermicity. Adsorption occurs almost spontaneously when it does not require substantial rearrangement of already-adsorbed CO but only by overcoming a considerable barrier when it does.

Using the Arrhenius equation, we estimated rate constants from the activation barriers in Figure 2, which we then used to approximate the CO coverage on each type of ensemble. Details of this calculation are included in the Supporting Information. The upshot is that under many experimentally and technologically relevant conditions, a significant fraction of Pd ensembles may be only "partially-poisoned". An ensemble is partially poisoned if it has at least one adsorbed CO molecule but fewer than the full number that the ensemble can accommodate. A partially poisoned dimer, for example, has exactly one adsorbed CO, whereas a partially poisoned tetramer may have one, two, or three. The presence of partially poisoned Pd ensembles is significant because in LH-type mechanisms, reaction is preceded by coadsorption of the reactants. O_2 is expected to undergo desorption easily (with no significant barrier) from sites near fully poisoned Pd ensembles without reaction with CO.

Figure 3 illustrates the oxidation mechanism of preadsorbed CO that we considered. It consists of three steps: (A) O_2 adsorption [$O_2(g) \rightarrow O_2(a)$], (B) OOCO formation [$O_2(a) + CO(a) \rightarrow OOCO(a)$], and (C) CO_2 formation and desorption [$OOCO(a) \rightarrow CO_2(g) + O(a)$]. In Table 1, we summarize predicted total energy changes (ΔE) and activation barriers (E_a) for each step. According to the results, molecular O_2 adsorption will be endothermic, whereas subsequent reaction steps tend to be highly exothermic. This suggests that the O_2 adsorption and activation step is rate-controlling and governs the oxidation process.

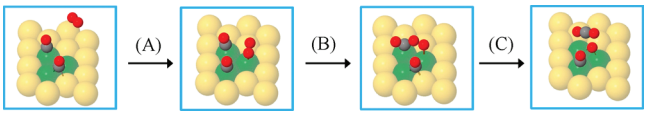

Figure 3. Illustration of the reaction of preadsorbed CO with O_2: (A) O_2 adsorption [$O_2(g) \rightarrow O_2(a)$], (B) OOCO formation [$O_2(a) + CO(a) \rightarrow OOCO(a)$], and (C) CO_2 formation/desorption [$OO-CO(a) \rightarrow CO_2(g) + O(a)$]. Red, yellow, green, and gray balls indicate O, Au, Pd, and C atoms, respectively.

In step (A), O_2 must be trapped on or near a CO-preadsorbed Pd ensemble to react successfully with a neighboring CO molecule. However, we find that desorption of O_2 from surface sites near poisoned Pd monomers is an almost nonactivated, downhill process (i.e, O_2 desorption barrier ~0.01 eV), implying that O_2 residence time on the surface near this ensemble may be too short for CO oxidation to occur. This would be consistent with a recent experimental observation[18] that isolated Pd sites are unlikely to catalyze O_2 dissociation and CO oxidation. Moreover, the facility with which O_2 is expected to desorb from sites adjacent to fully poisoned Pd monomers (by definition, the monomer cannot be partially poisoned) is characteristic of all of the fully poisoned Pd ensembles that we examined. Near partially poisoned Pd ensembles, sizable O_2 desorption barriers in the range of 0.06 to 0.23 eV are expected to exist; this suggests that these ensembles are capable of trapping O_2 for reaction with neighboring CO. In addition, our calculations show that the barrier for O_2 adsorption may also be a function of ensemble size and shape; the predicted adsorption barriers are 0.32 eV(D), 0.35 eV(TR_C), 0.50 eV(TR_L), 0.44 eV(TE_C), and 0.70 eV(TE_L) (Table 1). In view of the likely importance of trapped O_2 in CO oxidation, dimers and compact trimers are expected to provide more active sites than the other ensembles we examined because they have the lowest adsorption and highest desorption barriers for O_2.

In steps (B) [$O_2 + CO \rightarrow OOCO$] and (C) [$OOCO \rightarrow CO_2 + O$], CO_2 production occurs through a metastable OOCO intermediate that dissociates into CO_2 and O. A similar mechanism has been proposed for CO oxidation on pure Pd(111) and other metal surfaces (Au-based metal surfaces).[19] The OOCO formation reaction [(B)] is predicted to be exothermic by 0.15 to 0.50 eV with activation barriers of 0.15 to 0.27 eV, depending on the ensemble. According to our calculations, dissociation of OOCO into CO_2 and O exhibits only moderate barriers (0.18 to 0.32 eV) and very high exothermicities (2.02 to 2.46 eV) and so could occur rather easily at elevated temperatures; note that the O−O bond in OOCO is considerably stretched nearly to the peroxide state (~1.47 Å in O_2^{2-}). These results reinforce the importance of O_2 adsorption and activation. Once O_2 is activated on a CO-preadsorbed Pd ensemble, the subsequent reactions [(B) and (C)] can readily take place. The atomic O generated in step (C) of the reaction mechanism may also go on to participate in an oxidation reaction with absorbed CO. The predicted activation barrier of this reaction on the AuPd surface is 0.34 to 0.68 eV, depending on the ensemble.

Our study suggests that CO oxidation on AuPd catalysts may strongly depend on Pd ensemble size and shape; given this, it is

Table 1. Calculated Total Energy Changes (ΔE) and Activation Barriers (E_a in parentheses) in Each Reaction Step[a]

	(A) $O_2(g) \rightarrow O_2$	(B) $O_2 + CO \rightarrow OOCO$	(C) $OOCO \rightarrow CO_2 + O$
M	0.47 (0.48)	(N/A)[b]	(N/A)[b]
D	0.11 (0.32)	−0.15 (0.25)	−2.39 (0.18)
TR_C	0.15 (0.35)	−0.22 (0.26)	−2.46 (0.26)
TR_L	0.27 (0.50)	−0.31 (0.17)	−2.38 (0.25)
TE_C	0.38 (0.44)	−0.40 (0.27)	−2.38 (0.25)
TE_L	0.49 (0.70)	−0.50 (0.16)	−2.02 (0.32)

[a]All energy values are given in electronvolts [b]O_2 at the monomer site spontaneously desorbs off the surface without reacting with CO.

dx.doi.org/10.1021/jz201585q | J. Phys. Chem. Lett. 2012, 3, 566−570

important to understand the distribution of Pd ensembles in the surface layer. In the absence of adsorbates, Pd atoms tend to exist as isolated monomers surrounded by Au atoms, especially at low Pd coverage.[9,20] However, CO can also induce surface segregation due to the large differences in the strength of CO binding to various metals.[2,18,21] As we have seen, on the AuPd surface, CO preferentially binds to sites with higher Pd coordination (i.e., the order of CO binding strength is H > B > T, as shown in Figure 2). This site preference may under certain conditions provide a thermodynamic driving force for Pd agglomeration that counteracts the preference for monomers in the adsorbate-free surface.

Figure 4 compares the agglomeration energies of small Pd ensembles with and without a single adsorbed CO molecule.

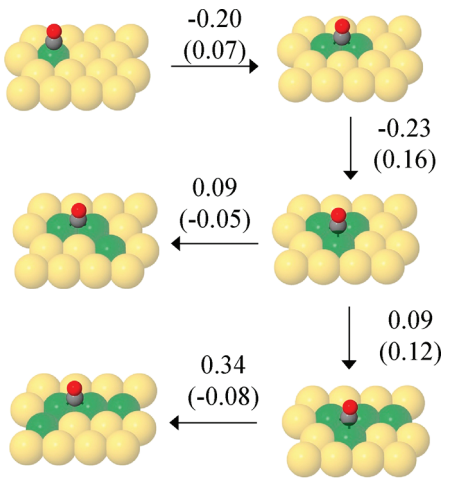

Figure 4. Calculated Pd agglomeration energies in the presence (ΔE_{CO}) or absence (ΔE in parentheses) of CO. The agglomeration energy is given by: for M + M → D, $\Delta E_{CO} = E_{slab}$(D-CO) + E_{slab}(Au/Pd) − E_{slab}(M-CO) − E_{slab}(M) and $\Delta E = E_{slab}$(D) + E_{slab}(Au/Pd) − 2E_{slab}(M). Here E_{slab}(D-CO) and E_{slab}(M-CO) indicate the total energies of CO-adsorbed dimer and monomer, respectively. E_{slab}(D) and E_{slab}(M) are the total energies of bare dimer and monomer, respectively, and E_{slab}(Au/Pd) is the total energy of Au overlayer on Pd(111). For other agglomeration energies, the similar calculation method can be applied. Big green and gold balls represent surface Pd and Au atoms, respectively, and small red and gray balls indicate respective O and C atoms in CO molecules. All energy values are given in electronvolts

Without adsorbed CO, the formation energies (on a per Pd atom basis) of the pictured Pd ensembles are seen to grow with ensemble size and also to be higher for more compact shapes, consistent with the fact that the Au−Pd interaction is energetically more favorable than the Pd−Pd interaction. When CO is added, portions of this trend are reversed. The two tetramers retain their positive agglomeration energies, indicating instability against division into smaller ensembles, but the agglomeration energies of D, TR_C, and TR_L all become negative, with the H site in TR_C pushing its formation energy below that of TR_L. Admittedly, the CO-induced surface restructuring of AuPd alloy nanoparticles used in actual catalytic processes is far more complex than presented here.[22] Nonetheless, our work at least reveals that the presence of CO significantly counteracts Pd dispersion in AuPd surfaces, as also evidenced by recent experiments;[22] from the results, we may reasonably expect a greater number of dimers and other, larger ensembles to form as a result. The adsorbate-induced agglomeration of Pd coupled to the ability of partially poisoned Pd ensembles (dimers and compact trimers, in particular) to trap and activate O_2 can be a plausible explanation for the enhanced activity of AuPd catalysts in CO oxidation. Moreover, considering that CO can be strongly bound to even small Pd ensembles, we speculate that the removal of adsorbed CO via oxidation may be one mechanism by which AuPd alloys resist CO poisoning.

In summary, DFT-GGA calculations were performed to examine the adsorption and oxidation of CO molecules on AuPd(111) alloy surfaces, particularly the effect of Pd ensemble size and shape. Our calculations demonstrate that CO predominantly adsorbs onto Pd atoms, and the adsorption energy is a strong function of CO coverage and Pd ensemble size and shape. This is mainly because of the strong dependence of CO adsorption strength on adsorption site type [hollow (H) > bridge (B) > on-top (T)]; that is, every Pd ensemble hosts a different assortment of T, B, and H sites due to differences in their sizes and shapes as well as CO coverage. Whereas the CO adsorption energy decreases with increasing coverage because of the gradual lack of favorable adsorption sites, the CO adsorption isotherm approximated using the Arrhenius equation suggests a significant fraction of small Pd ensembles may be only "partially-poisoned" under many experimentally and technologically relevant conditions. The "partially-poisoned" Pd ensembles tend to provide sites capable of trapping and activating O_2, leading to CO oxidation. Whereas the O_2 adsorption and activation step tends to be rate-controlling and governs the oxidation process, our study suggests that dimers and compact trimers would provide more active sites than the other ensembles we examined. Our calculations also demonstrate that the presence of CO could induce Pd agglomeration and yield more dimers and compact trimers compared to the adsorbate-free surface where monomers are prevailing, which may in turn facilitate CO oxidation. The mechanistic findings offer a plausible explanation on how Pd−Au alloy catalysts boost CO oxidation even at low temperatures and also lead us to speculate that CO removal through oxidation may be one mechanism by which AuPd alloys resist CO poisoning.

■ ASSOCIATED CONTENT

Ⓢ Supporting Information

Partially-poisoned fraction of each type of ensemble and predicted barriers in each CO+O_2 oxidations step at Pd dimer site, Pd linear trimer site, Pd compact trimer site, Pd linear tetramer site, and Pd compact tetramer site. This material is available free of charge via the Internet at http://pubs.acs.org.

■ AUTHOR INFORMATION

Corresponding Author

*E-mail: gshwang@che.utexas.edu.

Notes

The authors declare no competing financial interest.

■ ACKNOWLEDGMENTS

This work was supported by the R. A. Welch Foundation (F-1535). The authors also thank the Texas Advanced Computing Center for use of their computing resources.

REFERENCES

(1) Zhou, S. G.; McIlwrath, K.; Jackson, G.; Eichhorn, B. Enhanced CO Tolerance for Hydrogen Activation in Au-Pt Dendritic Heteroaggregate Nanostructures. *J. Am. Chem. Soc.* **2006**, *128*, 1780−1781.

(2) Gao, F.; Wang, Y. L.; Goodman, D. W. CO Oxidation over AuPd(100) from Ultrahigh Vacuum to Near-Atmospheric Pressures: The Critical Role of Contiguous Pd Atoms. *J. Am. Chem. Soc.* **2009**, *131*, 5734−5735.

(3) Xu, J.; White, T.; Li, P.; He, C. H.; Yu, J. G.; Yuan, W. K.; Han, Y. F. Biphasic Pd-Au Alloy Catalyst for Low-Temperature CO Oxidation. *J. Am. Chem. Soc.* **2010**, *132*, 10398−10406.

(4) Schmidt, T. J.; Jusys, Z.; Gasteiger, H. A.; Behm, R. J.; Endruschat, U.; Boennemann, H. J. On the CO Tolerance of Novel Colloidal PdAu/Carbon Electrocatalysts. *Electroanal. Chem.* **2001**, *501*, 132−140.

(5) Christoffersen, E.; Liu, P.; Ruban, A.; Skriver, H. L.; Norskov, J. K. Anode Materials for Low-Temperature Fuel Cells: A Density Functional Theory Study. *J. Catal.* **2001**, *199*, 123−131.

(6) Park, J. Y.; Zhang, Y.; Grass, M.; Zhang, T.; Somorjai, G. A. Tuning of Catalytic CO Oxidation by Changing Composition of Rh-Pt Bimetallic Nanoparticles. *Nano Lett.* **2008**, *8*, 673−677.

(7) Yuan, D. W.; Liu, Z. R.; Chen, J. H. Catalytic Activity of Pd Ensembles over Au(111) Surface for CO Oxidation: A First-Principles Study. *J. Chem. Phys.* **2011**, *134*, 054704/1−054704/7.

(8) Maroun, F.; Ozanam, F.; Magnussen, O. M.; Behm, R. J. The Role of Atomic Ensembles in the Reactivity of Bimetallic Electrocatalysts. *Science* **2001**, *293*, 1811−1814.

(9) Ham, H. C.; Hwang, G. S.; Han, J.; Nam, S. W.; Lim, T. H. On the Role of Pd Ensembles in Selective H_2O_2 Formation on PdAu Alloys. *J. Phys. Chem. C* **2009**, *113*, 12943−12945.

(10) Perdew, J. P.; Burke, K.; Ernzerhof, M. Generalized Gradient Approximation Made Simple. *Phys. Rev. Lett.* **1996**, *77*, 3865−3868.

(11) Kresse, G.; Furthmuller, J. *VASP the Guide*; Vienna University of Technology: Vienna, Austria, 2001.

(12) Blochl, P. E. Projector Augmented-Wave Method. *Phys. Rev. B* **1994**, *50*, 17953−17979.

(13) Henkelman, G.; Uberuaga, B. P.; Jonsson, H. a Climbing Image Nudged Elastic Band Method for Finding Saddle Points and Minimum Energy Paths. *J. Chem. Phys.* **2000**, *113*, 9901−9904.

(14) Ham, H. C.; Hwang, G. S.; Han, J.; Nam, S. W.; Lim, T. H. Geometric Parameter Effects on Ensemble Contributions to Catalysis: H_2O_2 Formation from H_2 and O_2 on AuPd Alloys. A First Principles Study. *J. Phys. Chem. C* **2010**, *114*, 14922−14928.

(15) Engel, T.; Ertl, G. Molecular-Beam Investigation of Catalytic Oxidation of CO on Pd(111). *J. Chem. Phys.* **1978**, *69*, 1267−1281.

(16) Li, Z. J.; Gao, F.; Tysoe, W. T. Carbon Monoxide Oxidation over Au/Pd(100) Model Alloy Catalysts. *J. Phys. Chem. C* **2010**, *114*, 16909−16916.

(17) Sakong, S.; Mosch, C.; Gross, A. O Adsorption on Cu-Pd Alloy Surfaces: Ligand versus Ensemble Effects. *Phys. Chem. Chem. Phys.* **2007**, *9*, 2216−2225.

(18) Gao, F.; Wang, Y. L.; Goodman, D. W. CO Oxidation over AuPd(100) from Ultrahigh Vacuum to Near-Atmospheric Pressures: CO Adsorption-Induced Surface Segregation and Reaction Kinetics. *J. Phys. Chem. C* **2009**, *113*, 14993−15000.

(19) Liu, Z. P.; Hu, P.; Alavi, A. Catalytic Role of Gold in Gold-Based Catalysts: A Density Functional Theory Study on the CO Oxidation on Gold. *J. Am. Chem. Soc.* **2002**, *124*, 14770−14779.

(20) Stephens, J. A.; Ham, H. C.; Hwang, G. S. Atomic Arrangements of AuPt/Pt(111) and AuPd/Pd(111) Surface Alloys: A Combined Density Functional Theory and Monte Carlo Study. *J. Phys. Chem. C* **2010**, *114*, 21516−21523.

(21) Andersson, K. J.; Calle-Vallejo, F.; Rossmeisl, J.; Chorkendorff, L. Adsorption-Driven Surface Segregation of the Less Reactive Alloy Component. *J. Am. Chem. Soc.* **2009**, *131*, 2404−2407.

(22) Alayoglu, S.; Tao, F.; Altoe, V.; Specht, C.; Zhu, Z.; Aksoy, F.; Butcher, D. R.; Renzas, R. J.; Liu, Z.; Somorjai, G. A. Surface Composition and Catalytic Evolution of Au_xPd_{1-x} (x = 0.25, 0.50, and 0.75) Nanoparticles Under CO/O_2 Reaction in Torr Pressure Regime and at 200 °C. *Catal. Lett.* **2011**, *141*, 633−640.